Production of good quality holograms by the THz pulsed vortex beams

Halima Benzehoua
Chouaib Doukkali University Faculty of Sciences: Universite Chouaib Doukkali Faculte des Sciences
Latifa Dalil-Essakali
Chouaib Doukkali University Faculty of Sciences: Universite Chouaib Doukkali Faculte des Sciences
Abdelmajid Belafhal (belafhal@gmail.com)
Chouaib Doukkali University https://orcid.org/0000-0003-2735-3108

Research Article

Keywords: THz pulsed vortex beams, Modulation depth, Frequency detuning, Holograms.

Posted Date: June 16th, 2021

DOI: https://doi.org/10.21203/rs.3.rs-334584/v1

Production of good quality holograms by the THz pulsed vortex beams

H. Benzehoua, L. Dalil-Essakali, A. Belafhal*

Laboratory LPNAMME, Laser Physics Group,

Department of Physics, Faculty of Sciences, Chouaïb Doukkali University,

P. B 20, 24000 El Jadida, Morocco

** Corresponding author. E-mail : belafhal@gmail.com*

Abstract

In this paper, we discuss the quality of holograms based on the calculation of the modulation depth. It's shown that the terahertz (THz) pulsed vortex beams play a vital role in holography filed, where two lasers with frequency difference have used. The THz vortex beams give new regions of larger frequency detuning and an important value of the modulation depth and fringe contrast (MDFC ratio) for obtaining the best holograms contrary to the Gaussian beams for which the best holograms are realized for small frequency detuning. The particular cases such as, Gaussian beam and single cycle pulses are deduced from our result. Numerical simulations are also presented to study the dependence of the MDFC ratio on the frequency detuning for THz vortex beams and Gaussian beams. This research could be beneficial in holographic interferometry, and it will firmly establish as a tool for scientific and engineering studies.

Keywords*: THz pulsed vortex beams; Modulation depth; Frequency detuning; Holograms.*

1. Introduction

THz technology is now widely used for extensive applications such as imaging with dispersive objects [1], detection of packaged integrated circuits [2], wireless communications [3,4], noninvasive diagnostics in biology and medicine [5-8], and noninvasive quality control and testing in industry [9-11]. Recently, considerable interests have been paid to study light beams with helical wave front. In modern optics, this kind of light is called vortex beams. Nowadays, optical vortex beams have been generated in various spectral ranges as examples; we cite THz [12], x-ray [13], millimeter [14], extreme ultraviolet [15], visible [16], and radio [17] ranges.

In recent years, the optical vortices have known a growing interest from the laser researchers due to their applications in many domains such as micromanipulations of particles

[18], atomic optics [19], photons entanglement states [20], optical metrology [21], binary optics and medical sciences [22]. The generation of optical vortex beams [23] has been developed using many different techniques, including computer-generated holograms [24-26], spatial light modulators [27-28], optical coordinate transformations [29], and fiber optics [30].

Many vortex beams had been introduced for the cylindrical symmetry, as examples, we cite the widely known Hypergeometric-Gaussian beams [31-33], Bessel-Gaussian beams [34-37] and Laguerre-Gaussian beams [38-40] that are separable in the polar coordinates. While, the well–known rectangular laser beams, which are separable inside the orthogonal direction including Four-petal Gaussian beams [41], Finite airy beams [42-43] and Hermite sinusoidal-Gaussian beams [44-48], are not originally vortex modes but they can be integrated by vortex phase amplitude.

On the other hand, the theory of holograms initially, called wave front reconstruction, since its invention by Gabor in 1948s [49], and the arrival of the laser at the beginning of the 1960s, has developed into a mature technology with a large variety of applications for which it is uniquely suited. In 1962, Leith and Upatnieks [50] combined Gabor's theory with their own work on side-reading radar and applied it to holography. In parallel with this work, Denisyuk [51] combined the basic idea of reconstruction of the wave front with the color photography method. Benton and Bove [52] discovered white-light transmission holography while researching holographic television at Polaroid Research Laboratories. Optical holography has attracted extensive attention, such as 3D display [53], optical metrology [54], medicine [55], and many more. In the optical holography technique, the hologram is an essential part that contains the complete information of the object beam.

In recent years, Odoulov et al. [56] have reported the recording of permanent holographic arrays using laser beams with a small frequency difference. In 2018, Malik and Escarquel [57] have proved that the best holograms can be obtained with significant frequency detuning. In 2020, Malik and Escarquel [58] showed also that dark hollow beams give more exact results than Gaussian beams for holography.

The present work aims to present, in a simple way that THz vortex beams present more precise results than Gaussian beams for holography. However, to the best of our knowledge, the modulation depth and fringe contrast ratio of THz vortex beams have not been studied elsewhere. The remainder of this manuscript is organized as follows: the theoretical calculation details for the MDFC ratio is developed in Section 2. Section 3 focuses on exploring the special

cases deduced from the laser beam. Then, Section 4 is devoted to the discussion of our results with numerical examples. Finally, the main results are outlined in the conclusion part.

2. Modulation depth of THz pulsed vortex pulses

In this section, we will evaluate the modulation depth of the considered pulses with two different colors. For that, we consider the interference of two THz pulsed vortex beams with two colors. Their electric fields are given by the following expression

$$E_1(r,t) = A_1 f(\mathrm{t})\cos(\omega_1 t - \vec{k}_1.\vec{r}), \tag{1.a}$$

and

$$E_2(r,t) = A_2 f(\mathrm{t})\cos(\omega_2 t - \vec{k}_2.\vec{r}), \tag{1.b}$$

where A_1 and A_2 are the amplitudes, ω_1 and ω_2 designate the angular frequencies, $\vec{k}_1$ and $\vec{k}_2$ represent the wave-vectors of the electric fields and $f(t)$ is the temporal profile given by [59]

$$f^2(t) = \left(\frac{\delta t}{\tau}\right)^{2\mathrm{n}} \mathrm{e}^{-\mathrm{t}^2/\tau^2}, \tag{2}$$

with τ is the pulse duration, n is an integer and δ is the controller parameter of the central dark spot size of the THz vortex pulse.

In time and space, from Eq. (1) we deduce the intensity distribution of the electric resulting field

$$\begin{aligned} I(\vec{r},t) &= \left|E_1(\vec{r},t) + E_2(\vec{r},t)\right|^2 \\ &= E_1(\vec{r},t)E_1^*(\vec{r},t) + E_2(\vec{r},t)E_2^*(\vec{r},t) + \left|E_1(\vec{r},t)E_1^*(\vec{r},t) + E_2(\vec{r},t)E_2^*(\vec{r},t)\right| \\ &= f^2(t)\left[\mathrm{A}_1^2 + \mathrm{A}_2^2 + 2\,\mathrm{A}_1\mathrm{A}_2\cos(\Omega\mathrm{t} - \vec{\mathrm{k}}.\vec{\mathrm{r}})\right], \end{aligned} \tag{3}$$

where $\Omega = \omega_2 - \omega_1$ and $\vec{k} = \vec{k}_2 - \vec{k}_1$ are the frequency detuning and the wave vectors of the fringe pattern, respectively. Eq. (3) can be written, in terms of the fringe contrast defined by $m = \dfrac{2\,\mathrm{A}_1\mathrm{A}_2}{\mathrm{A}_1^2 + \mathrm{A}_2^2}$, as

$$I(\vec{r},t) = (\mathrm{A}_1^2 + \mathrm{A}_2^2) f^2(t)\left[1 + m\cos(\Omega\mathrm{t} - \vec{\mathrm{k}}.\vec{\mathrm{r}})\right]. \tag{4}$$

By using Eq. (4), one evaluates a time-integrated pattern of the energy density per unit area by

$$\varepsilon(\vec{\mathrm{r}}) = \int_{-\infty}^{+\infty} I(\vec{r},t)dt\,. \tag{5}$$

Substituting in Eq. (5) the expression of the intensity distribution given by Eq. (4) and the temporal $f^2(t)$, one obtains

$$\varepsilon(\vec{\mathrm{r}}) = (\mathrm{I}_1 + \mathrm{I}_2)\left\{1 + M_d \cos(\vec{kr})\right\}, \tag{6}$$

which can be rearranged as

$$\varepsilon(\vec{\mathrm{r}}) = (A_1^2 + A_2^2)\int_{-\infty}^{+\infty} f^2(t)dt \left\{1 + \frac{m}{2}\frac{e^{-ikr}\int_{-\infty}^{+\infty} f^2(t)\,\mathrm{e}^{\mathrm{i}\Omega \mathrm{t}}dt + e^{ikr}\int_{-\infty}^{+\infty} f^2(t)\,\mathrm{e}^{-\mathrm{i}\Omega \mathrm{t}}dt}{\int_{-\infty}^{+\infty} f^2(t)dt}\right\}. \tag{7}$$

So, the modulation depth is given by

$$M_d = \frac{m}{2\cos(kr)}\frac{e^{-ikr}K^+ + e^{ikr}K^-}{K}, \tag{8}$$

where

$$K^+ = \left(\frac{\delta}{\tau}\right)^{2n}\int_{-\infty}^{+\infty} \mathrm{e}^{-\mathrm{t}^2/\tau^2}\, t^{2n}\, \mathrm{e}^{\mathrm{i}\Omega \mathrm{t}}\, dt\,, \tag{9.a}$$

$$K^- = \left(\frac{\delta}{\tau}\right)^{2n}\int_{-\infty}^{+\infty} \mathrm{e}^{-\mathrm{t}^2/\tau^2}\, t^{2n}\, \mathrm{e}^{-\mathrm{i}\Omega \mathrm{t}}\, dt\,, \tag{9.b}$$

and

$$K = \left(\frac{\delta}{\tau}\right)^{2n}\int_{-\infty}^{+\infty} \mathrm{e}^{-\mathrm{t}^2/\tau^2}\, t^{2n} dt\,. \tag{9.c}$$

By using the following identities [60]

$$\int_{-\infty}^{+\infty} x^m e^{\beta x^p} dx = \frac{\Gamma(\gamma)}{p\beta^\gamma}\,, \tag{10}$$

with $\gamma = \dfrac{m+1}{p}$, $Re\beta > 0$ and

$$\Gamma(\mathrm{n}+\tfrac{1}{2}) = \frac{(2n)!\sqrt{\pi}}{n!4^{\mathrm{n}}}\,, \tag{11}$$

where $\Gamma(.)$ is the gamma function, Eq. (9.c) can be written as follows

$$K = \tau\delta^{2n}\frac{(2n)!\sqrt{\pi}}{n!4^{\mathrm{n}}}. \tag{12}$$

For the evaluation of the integrals K^+ and K^-, we will use the following identity [61]

$$\int_{-\infty}^{+\infty} t^m e^{-pt^2+2qt} dt = \frac{e^{\frac{q^2}{p}}}{(2i\sqrt{p})^m}\sqrt{\frac{\pi}{p}}H_m\left(\frac{iq}{\sqrt{p}}\right), \tag{13}$$

where H_m is the Hermite polynomial.

After tedious algebraic calculations, Eqs. (9.a) and (9.b) can be expressed as

$$K^+ = e^{-\frac{\Omega^2\tau^2}{4}}\tau\sqrt{\pi}\left(\frac{\delta^2}{4}\right)^n (-1)^n H_{2n}\left(\frac{\Omega\tau}{2}\right), \tag{14}$$

and

$$K^- = e^{-\frac{\Omega^2\tau^2}{4}}\tau\sqrt{\pi}\left(\frac{\delta^2}{4}\right)^n (-1)^n H_{2n}\left(\frac{\Omega\tau}{2}\right). \tag{15}$$

Finally, the use of Eqs. (8), (12), (14) and (15) yields the expression of the modulation depth established as

$$M_d = me^{-\frac{\Omega^2\tau^2}{4}}\frac{n!}{(2n)!}\left|(-1)^n H_{2n}\left(\frac{\Omega\tau}{2}\right)\right|. \tag{16}$$

This last equation is a closed-form of the modulation depth of the THz pulsed vortex beams. In the following, we will investigate some particular cases of the considered beams and we will show that our result can generalized some previous works.

3. Particular cases

3.1 Case of Gaussian pulses

We examine now the particular case corresponding to n=0 and from Eq. (16) one deduces the modulation depth of these pulses given by

$$M_d^G = me^{-\frac{\Omega^2\tau^2}{4}}. \tag{17}$$

This result corresponds at that of the Gaussian pulse beams evaluated by Odoulov et al. [56].

3.2 Case of single cycle pulses

The temporal profile of these pulses is given by [59]

$$f^2(t) = \left(\frac{\delta t}{\tau}\right)^2 \mathrm{e}^{-\mathrm{t}^2/\tau^2}. \tag{18}$$

So, Eq. (16) can be written for n=1, as

$$M_d^{SCP} = \frac{m}{2}e^{-\frac{\Omega^2\tau^2}{4}}\left|\left(\frac{\Omega^2\tau^2}{4}-1\right)\right|. \tag{19}$$

This modulation depth depends on the following parameters: the fringe contrast, the frequency detuning and the pulse duration.

4. Numerical Simulations and discussions

In this part, we study the modulation depth and fringe contrast for the THz vortex beams and the Gaussian beams, of the temporal profile given by Eq. (2). So by using the main result established by Eq. (16), some numerical examples are performed to illustrate the MDFC ratio for the THz pulsed vortex beams in some plots in two views 3D or 2D, and we investigate some particular cases of the considered beams.

We illustrate in Fig. 1 the MDFC ratio for the particular case of the Gaussian pulses given by Eq. (17) as a function of the pulse duration τ and the frequency detuning Ω in tree-dimensional (x-y) plot.

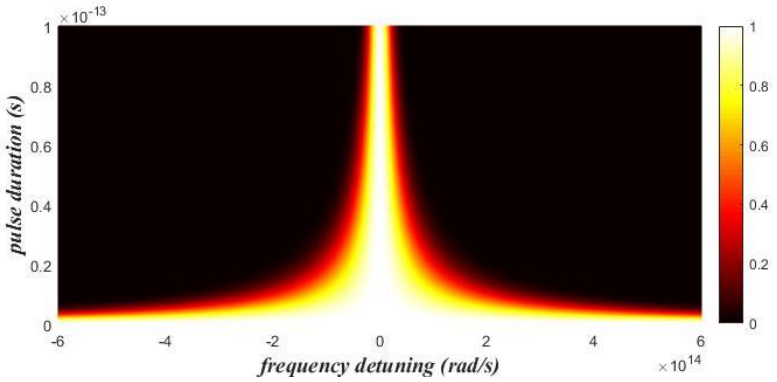

Figure 1: The MDFC ratio as a function of the pulse duration τ and frequency detuning Ω of the Gaussian pulses.

From this figure, one observes that the MDFC ratio increases from 0 to 1 as the color changes from black to white (see the rectangular bar). It can also be seen that the value of the MDFC ratio decreases when the pulse duration increases and the frequency detuning is larger for the Gaussian profile. Consequently, the appropriate value of the MDFC ratio is obtained for higher pulse duration and frequency difference.

In Fig. 2 the temporal profile of the THz vortex beams is depicted for different values of the beam order n by varying the controlled parameter δ. As be seen from this figure, the beam family keeps a similar shape profile and the same comportment when the beam order is changed. It is also observed from this plot, that the central dark spot of THz vortex beams increases and the dark region becomes wider with increasing n, and the width of the lobes begins to get smaller with the decreases of the skew parameter δ. Also, it can be seen that the intensity increases when the beam orders increase.

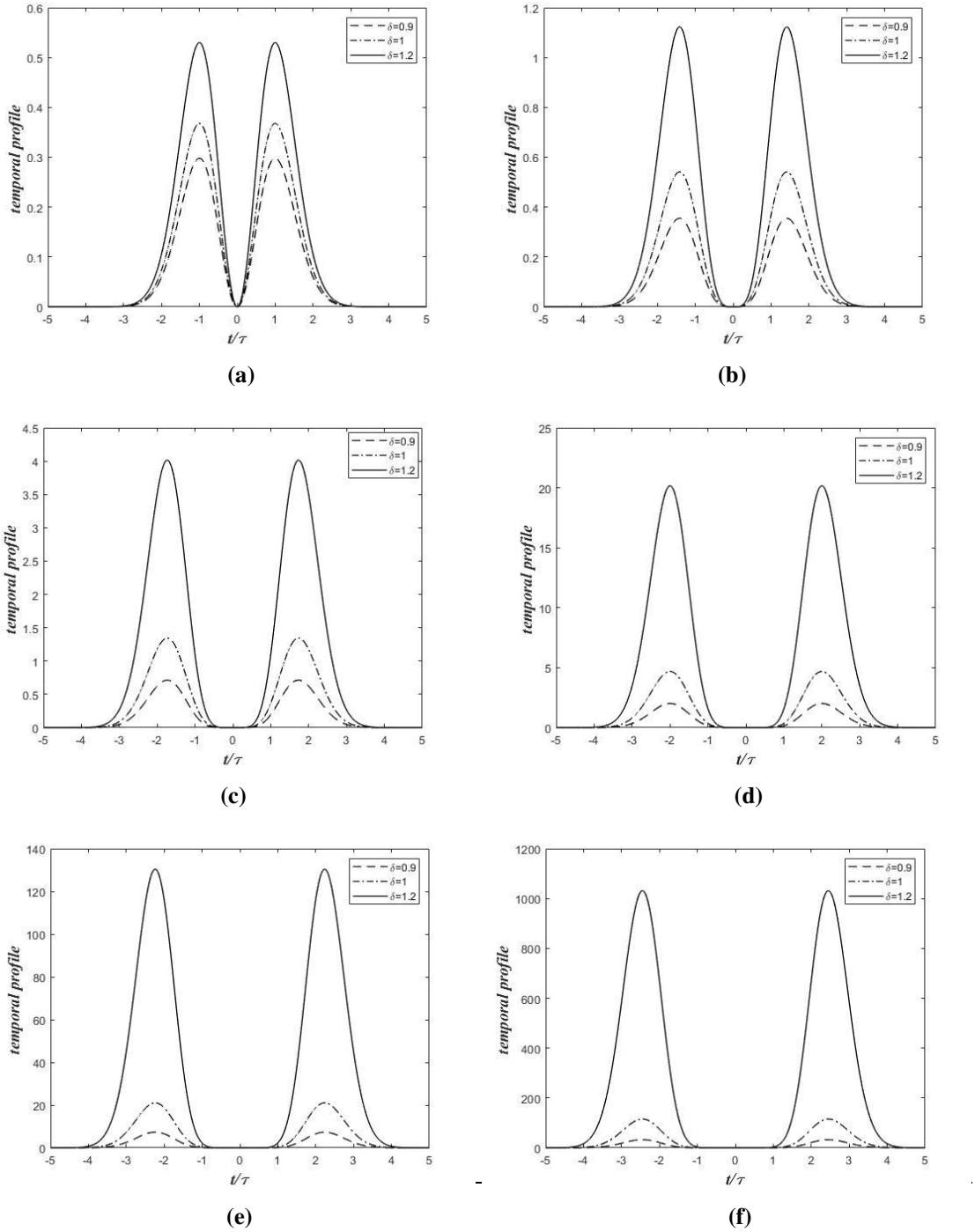

Figure 2: Temporal profile of THz vortex pulses for different skew parameters and for:
(a) n=1, **(b)** n=2, **(c)** n=3, **(d)** n=4, **(e)** n=5, and (**f**) n= 6.

To show the influence of the beam order and the skew parameter on the MDFC ratio, we give in Fig. 3 the variation of the MDFC ratio of THz vortex pulses as a function of the frequency detuning for three values of the pulse duration (τ=0.21 ps, 0.30 ps and 0.35 ps) and with different beam orders (n=1, 2, 3 and 4). From this figure, we can see clearly that the

increasing of the beam order n leads to the addition of the side lobes. For example, when n=2 and for τ=0.21 ps (see Fig. 3 (a)), we obtain two lobes, when n=3, we observe the apparition of another lobe (see Fig. 3 (b)). We can also note that when the pulse duration increases a slight increase occurs in the width of the lobes.

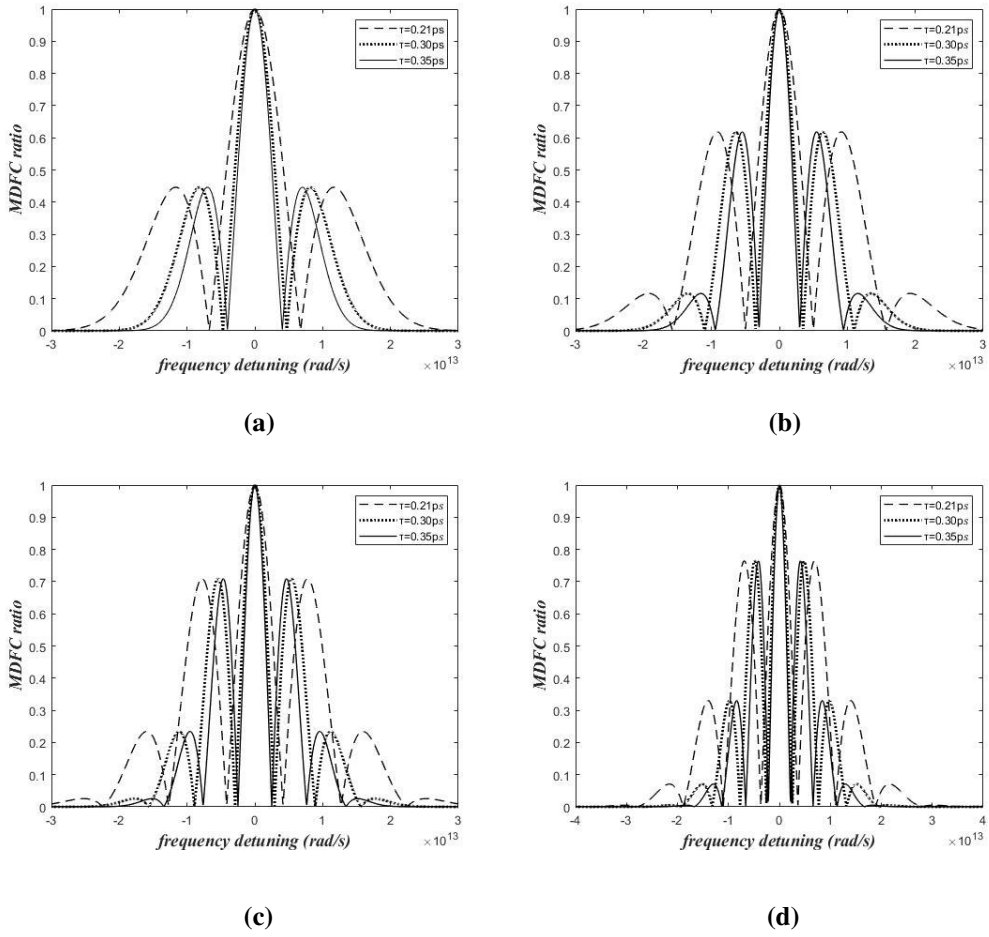

Figure 3: Behavior of the MDFC ratio of THz vortex pulses as a function of the frequency detuning for: **(a)** n=1, **(b)** n=2, **(c)** n=3 and **(d)** n=4.

The variation of the MDFC ratio as a function of the frequency detuning for the THz vortex beams profile (dashed curve) and the Gaussian beams profile (solid curve) is presented in Fig. 4 for different values of n (1, 2, 3 and 4) and two values of the pulse duration τ. It is clear from this figure that for the same frequency detuning, the MDFC ratio of the THz vortex beams is much higher compared to that one of the Gaussian beams (red hatched area). We can also observe the appearance of side lobes for the THz vortex beams which increase with the increase of the beam order n. We note that the total number of side lobes is proportional to the

order of the studied profile. However, the MDFC ratio presents a slight increase when the pulse duration τ increases.

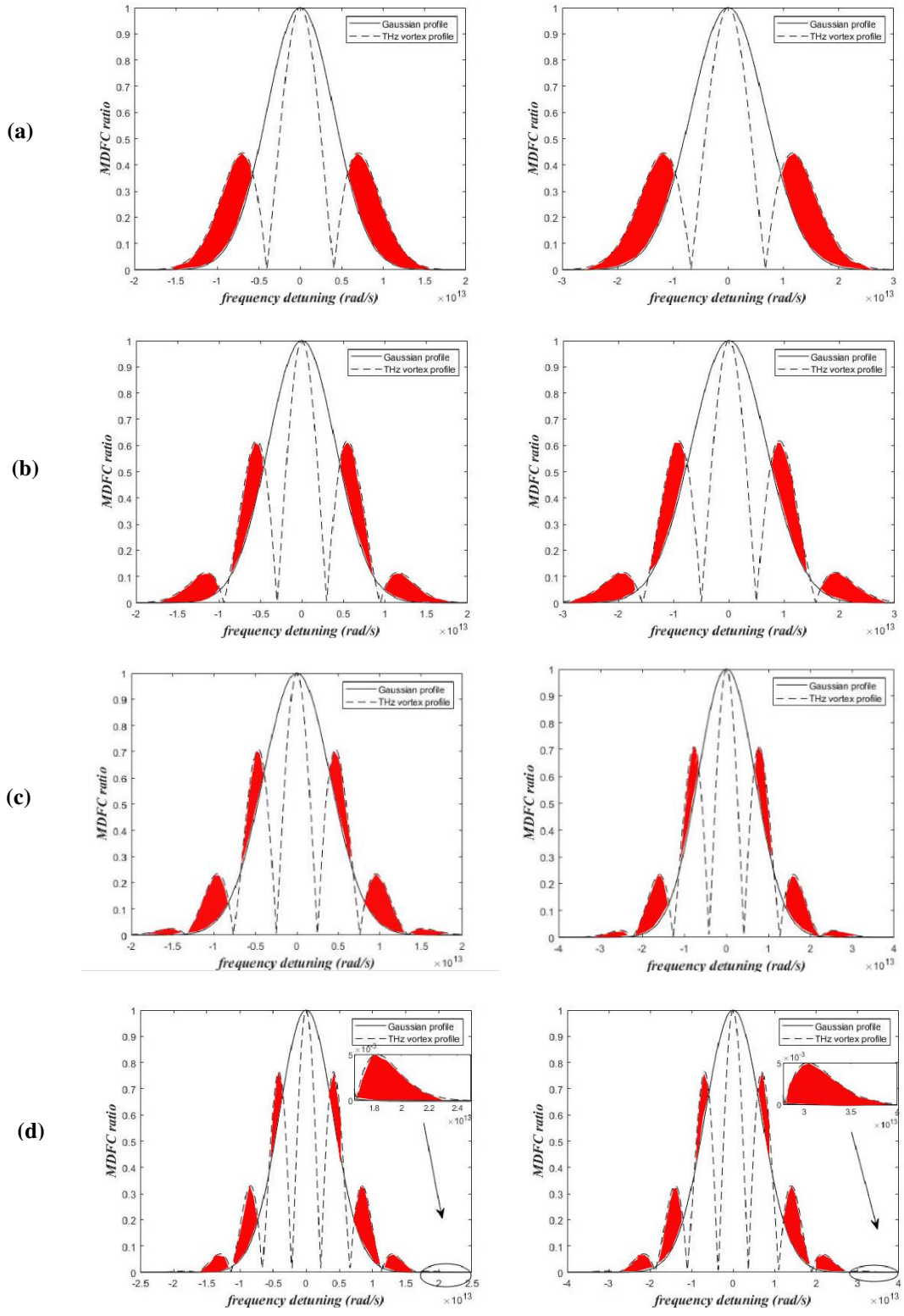

Figure 4: The MDFC ratio as a function of the frequency detuning for two values of the pulse duration set as τ = 0.21 ps and τ = 0.35 ps and (**a)** n=1, **(b)** n=2, **(c)** n=3 and **(d)** n=4.

In Fig. 5, we illustrate the MDFC ratio for THz pulsed vortex beams as a function of the pulse duration τ and the frequency detuning Ω for and different values of the beam order n.

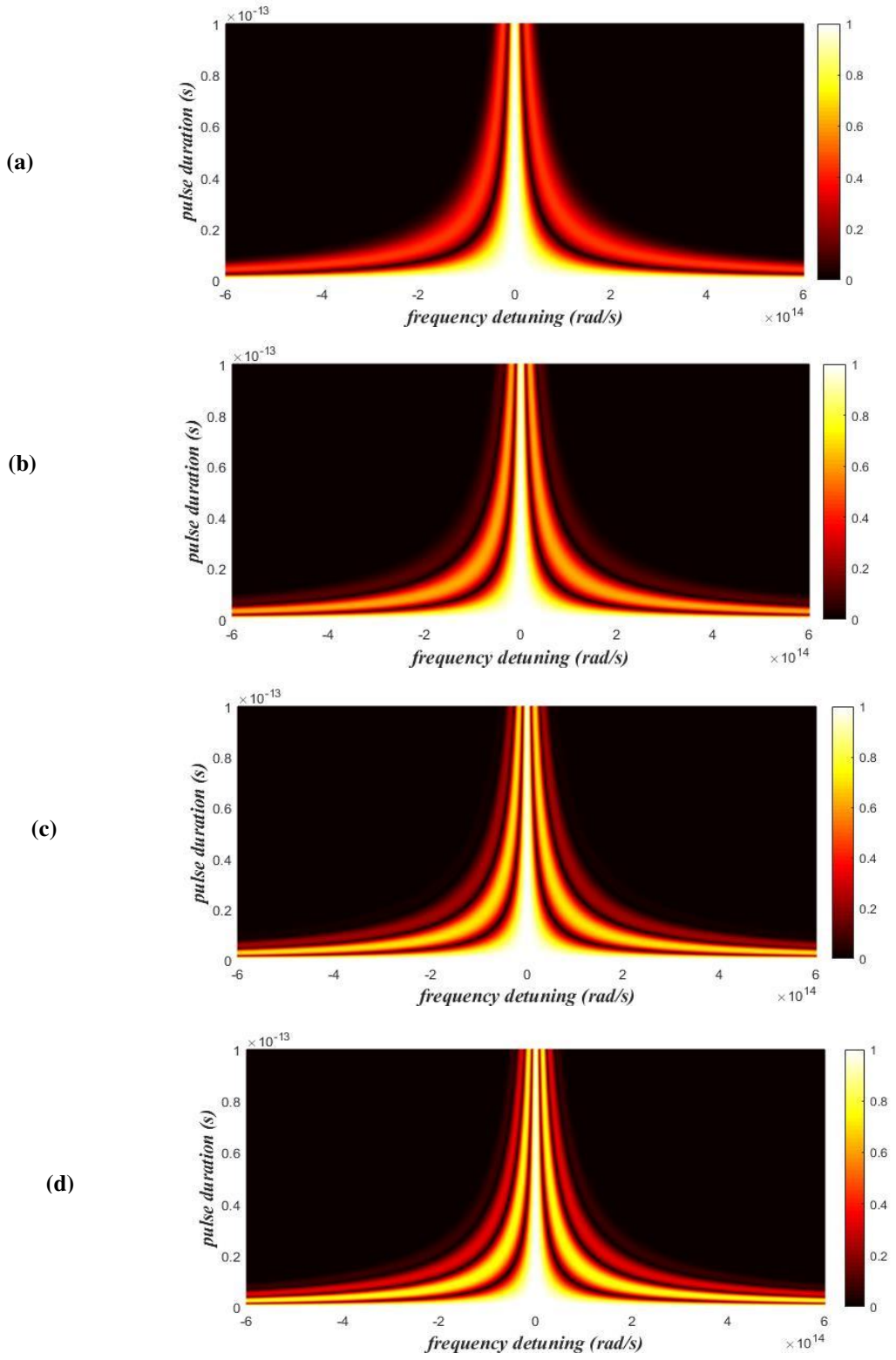

Figure 5: The MDFC ratio as a function of the pulse duration τ and the frequency detuning of the THz vortex beams for **(a)** n=1, **(b)** n=2, **(c)** n=3 and **(d)** n=4.

The rectangular bar shows the increase of the MDFC ratio from 0 to 1 as the color changes from black to white. It's noted that the MDFC ratio gradually decreases as the frequency detuning increases and then a thin strip is formed while the MDFC ratio keeps null. In the end and as Ω increases further, the MDFC ratio begins to enhance and gradually decreases to zero, which results the appearance of two null regions (Fig. 5 (a)) favoring the formation of the holograms. We can observe that by increasing the beam order n, the new thin strips appear (Figs. 5(b)-(d)). Hence, the MDFC ratio of the THz pulsed vortex beams presents discontinuities compared to that one of the Gaussian profile, due to the formation of null region (MDCD ratio = 0). The increasing of the beam order n leads to increase the discontinuities and a better quality of the hologram can be obtained for this beams family.

5. Conclusion

In this paper, we have investigated a THz vortex beam profile showing its important role in holography where two lasers with frequency difference are used. Based on the expression of the modulation depth, we have revealed that a hologram quality can be improved by adjusting the beam profile parameter. We can conclude that the THz vortex beams profile, contrary to the Gaussian beams profile, offers a new area where best quality holograms can be produced for higher frequency detuning. We believed that the present work is valuable for investigations of THz vortex beams in the holographic interferometry field.

References

[1] M.S. Kulya, N.S. Balbekin, I.V. Gredyuhina, M.V. Uspenskaya, A.P. Nechiporenko, N.V. Petrov, “Computational terahertz imaging with dispersive objects,” J. Mod. Opt., 64 (2017) 1283-1288.

[2] K. Ahi, S. Shahbazmohamadi, N. Asadizanjani, “Quality control and authentication of packaged integrated circuits using enhanced spatial-resolution terahertz time-domain spectroscopy and imaging,” Opt. Lasers Eng., 104 (2018) 274-284.

[3] T. Nagatsuma, G. Ducournau, C.C. Renaud, “Advances in terahertz communications accelerated by photonics,” Nat. Photonics, 10 (2016) 371-379.

[4] V. Semenova, V. Bespalov, “Terahertz technologies,” Photonics, 51 (2015) 126-141.

[5] Q. Sun, Y. He, K. Liu, S. Fan, E.P.J. Parrott, E. Pickwell, M. Pherson, “Recent advances in terahertz technology for biomedical applications,” Quantum Imaging Med. Surg., 7 (2017) 345-355.

[6] X. Yang, X. Zhao, K. Yang, Y. Liu, Y. Liu, W. Fu, Y. Luo, “Biomedical applications of terahertz spectroscopy and imaging,” Trends Biotechnol., 34 (2016) 810-824.

[7] N.S. Balbekin, Y.V. Grachev, S.V. Smirnov, V.G. Bespalov, “The versatile terahertz reflection and transmission spectrometer with the location of objects of researches in the horizontal plane,” J. Phys. Conf. Ser., 584 (2015) 012010-012015.

[8] M.V. Duka, L.N. Dvoretskaya, N.S. Babelkin, M.K. Khodzitskii, S.A. Chivilikhin, O.A. Smolyanskaya, “Numerical and experimental studies of mechanisms underlying the effect of pulsed broadband terahertz radiation on nerve cells,” Quant. Electron., 44 (2014) 707-712.

[9] C.D. Stoik, M.J. Bohn, J.L. Blackshire, “Nondestructive evaluation of aircraft composites using transmissive terahertz time domain spectroscopy,” Opt. Exp., 16 (2008) 17039-17051.

[10] K. Ahi, M. Anwar, “Advanced terahertz techniques for quality control and counterfeit detection,” Proc. SPIE, 9856 (2016) 98560G-1-14.

[11] N.S. Balbekin, E.V. Novoselov, P.V. Pavlov, V.G. Bespalov, N.V. Petrov, “Nondestructive monitoring of aircraft composites using terahertz radiation,” Proc. SPIE, 9448 (2015) 94482D-1-8.

[12] J. He, X. Wang, D. Hu, J. Ye, S. Feng, Q. Kan, Y. Zhang, “Generation and evolution of the terahertz vortex beam,” Opt. Exp., 21 (2013) 20230–20239.

[13] A.G. Peele, P.J. McMahon, D. Paterson, C.Q. Tran, A. P. Mancuso, K.A. Nugent, J.P. Hayes, E. Harvey, B. Lai, I. McNulty, “Observation of an x-ray vortex,” Opt. Lett., 27 (2002) 1752-1759.

[14] Y. Yan, G. Xie, M.P.J. Lavery, H. Huang, N. Ahmed, C. Bao, Y. Ren, Y. Cao, L. Li, Z. Zhao, A.F. Molisch, M. Tur, M.J. Padgett, A.E. Willner, "High-capacity millimeter-wave communications with orbital angular momentum multiplexing," Nat. Commun., 5 (2014) 4876-4885.

[15] R. Géneaux, A. Camper, T. Auguste, O. Gobert, J. Caillat, R. Taïeb, T. Ruchon, "Synthesis and characterization of attosecond light vortices in the extreme ultraviolet," Nat. Commun., 7 (2016) 12583-12583.

[16] X. Cai, J. Wang, M.J. Strain, B. Johnson-Morris, J. Zhu, M. Sorel, J.L. O'Brien, M.G. Thompson, S. Yu, "Integrated compact optical vortex beam emitters," Science, 338 (2012) 363-366.

[17] S. Yu, L. Li, G. Shi, C. Zhu, X. Zhou, Y. Shi, "Design, fabrication, and measurement of reflective metasurface for orbital angular momentum vortex wave in radio frequency domain," Appl. Phys. Lett., 108 (2016) 121903-121909.

[18] J. Arlt, V. Garcez-Chavez, W. Sibbett, K. Dholakia, "Optical micromanipulation using Bessel light beam," Opt. Commun., 197 (2001) 239-245.

[19] H. Ito, T. Nakata, K. Sakaki, M. Ohtsu, K. Lee, W. Jhe, "Laser spectroscopy of atoms guided by evanescent waves in micron-sized hollow opticalfFibers," Phys. Rev. Lett., 76 (1996) 4500-4503

[20] A. Mair, A. Vaziri, G. Weihs, A. Zeilinger, "Entanglement of the orbital angular momentum states of photons," Nature, 412 (2001) 313-316.

[21] J. K. Gasvik. Optical Metrology. (John Wiley & Sons, 2003).

[22] K.T. Gahagan, G.A. Swartz lander, "Optical vortex trapping of particles," Opt. Lett., 21 (1996) 827-829.

[23] J. Yin, W. Gao, Y. Zhu, "Generation of dark hollow beam and their applications," Prog. Opt., 44 (2003) 1158-1169.

[24] A. Vasara, J. Turunen, A.T. Friberg, "Realization of general non-diffracting beams with computer generated holograms," J. Opt. Soc. Am. A, 6 (1989) 1748-1754

[25] A.V. Carpentier, H. Michinel, J.R. Salgueiro, D. Olivieri, "Making optical vortices with computer-generated holograms," Am. J. Phys., 76 (2008) 916-921.

[26] N.R. Heckenberg, R. McDuff, C.P. Smith, A.G. White, "Generation of optical phase singularities by computer-generated holograms," Opt. Lett., 17 (1992) 221-223.

[27] D. McGloin, G. Spalding, H. Melville, W. Sibbet, K. Dholakia, "Applications of spatial light modulators in atom optics," Opt. Exp., 11 (2003) 158-166.

[28] J.A. Davis, E. Carcole, D.M. Cottrell, “Intensity and phase measurements of nondiffracting beams generated with a magneto-optic spatial light modulator,” Appl. Opt., 35 (1996) 593-598.
[29] N. Davidson, A.A. Friesem, E. Hasman, “Optical coordinate transformations,” Appl. Opt., 31 (1992) 1067-1073.
[30] S. Ramachandran, P. Kristensen, M.F. Yan, “Generation and propagation of radially polarized beams in optical fibers,” Opt. Lett., 34 (2009) 2525-2527.
[31] V.V. Kotlyar, R.V. Skidanov, S.N. Khonina, V.A. Soifer, “Hypergeometric modes,” Opt. Lett., 32 (2007) 742-744.
[32] E. Karimi, G. Zito, B. Piccirillo, L. Marrucci, E. Santamato, “Hypergeometric Gaussian modes,” Opt. Lett., 32 (2007) 3052-3055.
[33] R.V. Skidanov, S.N. Khonina, A.A. Morosov, “Optical rotation of microparticles in hypergeometric laser beams with a diffractive optical element with multilevel microrelief,” J. of Opt. Techn., 80 (2013) 585-589.
[34] J. Arlt, K. Dholakia, “Generation of higher-order Bessel beams by use of an axicon,” Opt. Commun., 177 (2000) 297-301.
[35] D. McGloin, K. Dholakia, “Bessel beams: diffraction in new light,” Contemp. Phys., 46 (2005) 15-28.
[36] V.V. Kotlyar, A. Kovalev, S.N. Khonina, R.V. Skidanov, V.A. Soifer, H. Elfstrom, N. Tossavainen, J. Turenen, “Diffraction of conic and Gaussian by spiral phase plate,” Appl. Opt., 45 (2006) 2656-2665.
[37] P. Vaity, L. Rusch, “Perfect vortex beam: Fourier transform of Bessel beam,” Opt. Lett., 40 (4) (2015) 742-744.
[38] L. Allen, M.W. Beijersbergen, R.J. Spreeuw, J. P. Woerdman, “Orbital angular momentum of light and the transformation of Laguerre-Gaussian modes,” Phys. Rev. A, 45 (1992) 8185-8189.
[39] S.A. Kennedy, M.J. Szabo, H. Teslow. J.Z. Porterfield, E.R.I. Abraham, “Creation of Laguerre-Gaussian laser modes using diffractive optics,” Phys. Rev. A, 66 (2002) 043801-043806.
[40] G. Vallon, “On the properties of circular beams: normalization, Laguerre-Gauss, and free-space propagation,” Opt. Lett., 40 (2015) 1717-1722.
[41] K. Duan, B. Lü, “Four-petal Gaussian beams and their propagation,” Opt. Commun., 261 (2006) 327-331.

[42] G.A. Siviloglou, J. Broky, A. Dogariu, D.N. Christodoulides, "Observation of accelerating Airy beams," Phys. Rev. Lett., 99 (2007) 213901-213904.
[43] G.A. Siviloglou, D.N, Christodoulides, "Accelerating finite Airy beams," Opt. Lett., 32, (2007) 979-981.
[44] L.W. Casperson, A.A. Tovar, "Hermite-Sinusoidal-Gaussian beams in complex optical systems," J. Opt. Am. A, 15 (1998) 954-961.
[45] A.A. Tovar, L.W. Casperson, "Production and propagation of Hermite-sinusoidal-Gaussian laser beams," J. Opt. Am. A, 15 (1998) 2425-2432.
[46] A. Belafhal, M. Ibnchaikh, "Propagation properties of Hermite-cosh-Gaussian laser," Opt. Commun., 186 (2000) 269-276.
[47] Z. Hricha, A. Belafhal, "Focusing properties of focal Hermite-cosh-Gaussian beams," Opt. Commun., 253 (2005) 242-249.
[48] S. Chib, L. Dalil-Essakali, A. Belafhal, "Propagation properties of a novel generalized flattened Hermite-Cosh-Gaussian light beam," Opt. Quant. Electron., 52 (2020) 277-290.
[49] D. Gabor, "A new microscopic principle," Nature, 161 (1948) 777–778.
[50] E.N. Leith, J. Upatnieks, "Reconstructed wave fronts and communication theory," J. Opt. Soc. Am. A, 52 (1962) 1123-1131.
[51] Y.N. Denisyuk, "Photographic reconstruction of the optical properties of an object in its own scattered radiation field," Soviet. Phys. Doklady, 7 (1962) 543-545.
[52] S.A. Benton, V.M. Bove Jr. Holographic imaging. (John Wiley & Sons 2008).
[53] U. Schnars, W. Jueptner, "Direct recording of holograms by a CCD target and numerical reconstruction," Appl. Opt., 33 (1994) 179-181.
[54] T. Kreis. Handbook of holographic interferometry: optical and digital methods. First ed., (Wiley-VCH, Weinheim, 2005).
[55] K. Boyer, J. Solem, J. Longworth, A. Borisov, C. Rhodes, "Biomedical three-dimensional holographic microimaging at visible, ultraviolet and X-ray wavelengths," Nat. Med., 2 (1996) 939-941.
[56] S. Odoulov, A. Shumelyuk, H. Badorreck, S. Nolte, K.M. Voit, M. Imlau, "Interference and holography with femtosecond laser pulses of different colors," Nat. Commun., 6 (2015) 5866-5873.
[57] L. Malik, A. Escarquel, "Role of the temporal profile of femtosecond lasers of two different colors in holography," EPL, 124 (2018) 64002 (1-6).

[58] L. Malik, A. Escarquel, “Dark hollow lasers may be better candidates for holography,” Optics and Laser Technology, 132 (2020) 106485-106491.
[59] Y.A. Kapoyko, A.A. Drozdov, S.A. Kozlov, X.C. Zhang, “Evolution of few-cycle pulses in nonlinear dispersive media: Velocity of the center of mass and root-mean-square duration,” Phys. Rev. A., 94 (2015) 033803-033812.
[60] I.S. Gradshteyn, I.M. Ryzhik. Table of integrals, series, and products. 7th ed, Academic Press, (Amsterdam; Boston, 2007).
[61] A. Belafhal, Z. Hricha, L. Dalil-Essakali, T. Usman, “A note on some integrals involving Hermite polynomials encountered in caustic optics,” Adv. Math. And Appl., 5 (3) (2020) 313-319.